Quantum Information Processing (2023) 22:229
https://doi.org/10.1007/s11128-023-03969-4

Exploring quantum correlations of two-qubit Heisenberg chain model influenced by magnetic dipole–dipole, magnetic field, and a symmetric cross interaction

M. Youssef[1] · S. I. Ali[1] · M. Y. Abd-Rabbou[1] · A. -S. F. Obada[1]

Received: 9 January 2023 / Accepted: 14 April 2023

Abstract
The concepts of concurrence, 3-steerability, and Clauser–Horne–Shimony–Holt (CHSH) inequality are employed to investigate the environmental impacts on the quantum correlations of the two-spin-1/2 Heisenberg XYZ chain model. In particular, the effects of a homogeneous magnetic field, symmetric cross interaction, and dipole–dipole interaction on the entanglement, degree of steerability, and non-locality are discussed. Results show that the entanglement and steering phenomena are bounded by the non-locality for both positive and negative values of dipole–dipole coupling. It has also been observed that higher symmetric cross-interaction strengthens the quantum correlations, whereas the homogeneous magnetic field weakens the quantumness of the system. The findings indicate that a magnetic field normal to the magnetic dipole yields better quantum correlations than when they are parallel.

Keywords Quantum correlation · Steering · Non locality · Concurrence

1 Introduction

The study of the magnetic and spin structures of low-dimensional magnets has become increasingly important due to its potential applications in condensed matter physics [1, 2]. Numerous computations of magnetic anisotropies, Ising interactions (both square and dipolar), and long-range dipolar interactions have been conducted [3–5]. The two-dimensional Heisenberg chain model and dipolar Ising model with the external magnetic field have been studied in detail [6–8]. The Dzyaloshinsky-Moriya (DM) interaction, which is responsible for weak ferromagnetism or helimagnetism, is particularly crucial in systems which lack spatial reversal symmetry [9, 10]. The anti-symmetric Dzyaloshinsky-Moriya (DM) interaction is responsible for the emergence

✉ S. I. Ali
salama5laser@azhar.edu.eg

[1] Mathematics Department, Faculty of Science, Al-Azhar University, Nassr City, Cairo 11884, Egypt

Published online: 03 June 2023

of magnetization in a system [11, 12]. On the other hand, the Kaplan-Shekhtman-Entin-Wohlman-Aharony (KSEA) interaction, which is a symmetric mixed term, is responsible for weak ferromagnetism [11, 12]. The quantum correlation of the Heisenberg chain model in the presence of the KSEA interaction has been discussed [13]. Further the degree of estimation of the KSEA interaction by using quantum Fisher information has been explored [14]. Moreover, the dipole–dipole character of certain substances can result in strong magnetic interactions, while exchange and indirect interactions tend to be relatively weak [15]. The presence of dipole–dipole interaction and symmetric KSEA interaction can lead to the encoding of information, while the rate of the two interactions can determine the extent of this encoding [16].

On the other side, characterizing quantum correlations is an essential part of many quantum information and computation tasks. Entanglement between quantum states is an especially intriguing resource for both fundamental physics and applications [17]. Several mathematical functions have been proposed to measure the entanglement, such as concurrence, negativity, logarithmic negativity, and entanglement of formation [18–20]. Among the applications of entanglement we may mention quantum key distribution, quantum computing, and quantum teleportation [21]. The entanglement of different paramagnetic materials and an open alternating chain of nuclear spins s = 1/2 with spin-spin couplings have been studied [22, 23]. Also, the entanglement of Heisenberg chain models [24–26], light-matter interactions [27, 28], and quantum dot systems [29, 30] have been witnessed. Another indicator of quantum correlations is the steering between bipartite quantum systems. This measure was introduced by Schrödinger in 1935 [31]. In particular, numerous inequalities have been formulated for both continuous- and discrete-variable quantum systems, to study the phenomenon of quantum steering [32–35]. Investigations into the steerability of Heisenberg models at finite temperatures, bipartite two-qubit X-states, two-level or three-level detectors in a non-Markovian environment have been conducted [36–40]. In addition, non-locality of quantum states is characterized by the violation of Bell inequalities - the simplest of which being the Clauser Horne Shimony Holt (CHSH) form [41]. Further, non-locality has been quantified through the use of uncertainty-induced quantum non-locality [42], Bell non-locality [43], and measurement-induced non-locality [44].

The aim of our research is to explore a composite system of the XYZ Heisenberg chain model, which features magnetic dipole–dipole interactions, an external field, and a symmetric KSEA interaction. This model is capable of exhibiting a wide range of quantum phenomena and provides an opportunity to analyze the intricate interplay between different types of interactions, as well as how they affect entanglement and quantum correlations. Through our study of this model, we can gain valuable insight into core questions concerning quantum correlation, such as how entanglement is created and controlled. By utilizing numerical simulations and analytical techniques, we hope to demonstrate the power of quantum information theory to identify and understand the effects of various interactions, which could lead to new and interesting applications in both computational physics and condensed matter.

The paper is organized as follows:- We begin by briefly introducing the mathematical forms of three quantum quantifiers, namely: quantum concurrence, 3-steerability, and normalized CHSH-non-locality in the next section. Section 3 discusses the different parts of the Hamiltonian for the physical model and presents the exact solution

of the Hamiltonian. Additionally, we examine the impact of magnetic fields and symmetric cross-interactions on the three quantum quantifiers for different positions of the dipoles direction. Finally, we conclude with a summary of our results.

2 Preliminaries

This section provides a brief review of the mathematical formulas associated with quantum non-separability, steerability, and non-locality, based on the concepts of concurrence, 3-steerability and CHSH-non-locality.

2.1 Concurrence

In a bipartite density mixed state $\hat{\rho}_{AB}$, the quantification of entanglement (non-separability) is efficiently achieved through the utilization of the concurrence, made mathematically accessible by Wootters' formula [19], given as follows:

$$\mathcal{E} = \max\left\{0, \sqrt{\lambda_1} - \sqrt{\lambda_2} - \sqrt{\lambda_3} - \sqrt{\lambda_4}\right\},\ \lambda_1 \geq \lambda_2 \geq \lambda_3 \geq \lambda_4 \geq 0. \tag{1}$$

where, λ_i represent the eigenvalues of the non-Hermitian operator $\rho_{AB}(\sigma_y \otimes \sigma_y)\rho^*_{AB}(\sigma_y \otimes \sigma_y)$, while ρ^*_{AB} is the complex conjugated of ρ_{AB}. It is noteworthy that the concurrence of a fully entangled state is equal to 1, whereas separable mixed states exhibit a vanishing concurrence.

2.2 Steering

The fundamental definition of steering phenomenon goes back to the paradoxical aspects of quantum mechanics investigated by Einstein-Podolsky-Rosen and Schrödinger. Later the idea of steering phenomenon was precisely formulated for discrete observables, and established as an intermediate between non-separability and non-locality [32]. Remarkably, one of the most effective indicators of steering lies in the 3-steerability, which be defined for arbitrary density states such as ρ_{AB} with an X-shaped structure, in the form [45],

$$\mathcal{S} = \max\left\{0, \frac{||\vec{c}|| - 1}{\sqrt{3} - 1}\right\}, \tag{2}$$

where, $\vec{c} = \{c_1, c_2, c_3\}$, with $c_i = Tr[\rho_{AB}\sigma_i \otimes \sigma_i]$, $||\vec{c}|| \geq 1$, and $\sqrt{3}$ is taken to normalize the degree of steerability and obtained from the maximum violation of steering inequality.

2.3 CHSH-non-locality

To gain a more profound understanding of quantum correlations, it is essential to derive the Bell–Clauser–Horne–Shimony–Holt (CHSH) inequality. To assess CHSH

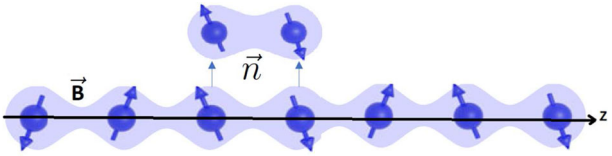

Fig. 1 A Sketch of an XYZ Heisenberg chain model, where we choose an arbitrary two qubits that have a position vector $\vec{n}$ and are influenced by a symmetric cross interaction Γ, and a uniform external magnetic field $\vec{B}$

non-locality, the Bell operator associated with the CHSH inequality, can be employed as presented in [46]. Accordingly the Bell-CHSH inequality is defined as follows,

$$\beta_{CHSH} = \mathbf{a}.\boldsymbol{\sigma}_A \otimes (\mathbf{b} + \mathbf{b}').\boldsymbol{\sigma}_B + \mathbf{a}'.\boldsymbol{\sigma}_A \otimes (\mathbf{b} - \mathbf{b}').\boldsymbol{\sigma}_B \tag{3}$$

where, $\mathbf{a}, \mathbf{a}', \mathbf{b}, \mathbf{b}'$ are unit vectors. For an arbitrary two-qubit with X-shaped, the convenient normalization of the maximal violation of the CHSH inequality is expressed as,

$$\mathcal{B} = \max\left\{0, \frac{\max Tr[\beta_{CHSH}\rho_{AB}] - 2}{2\sqrt{2} - 2}\right\}, \tag{4}$$

where, $2\sqrt{2}$ is the maximum value of CHSH inequality obtained according to the pure maximal entangled states.

3 Physical model

Let us consider a physical model characterizing a two-qubit XYZ Heisenberg chain that is influenced by a symmetric cross interaction, a uniform external magnetic field, and a magnetic dipole–dipole interaction. This model is sketched in Fig. 1, and its Hamiltonian can be written as,

$$\hat{H} = \hat{\mathcal{H}}_I + \hat{\mathcal{H}}_S + \hat{\mathcal{H}}_M + \hat{\mathcal{H}}_D. \tag{5}$$

Here, $\hat{\mathcal{H}}_I$ is the Hamiltonian of a two-qubit XYZ Heisenberg chain model, which is given by [47],

$$\hat{\mathcal{H}}_I = J_x\hat{\sigma}_a^x\hat{\sigma}_b^x + J_y\hat{\sigma}_a^y\hat{\sigma}_b^y + J_z\hat{\sigma}_a^z\hat{\sigma}_b^z, \tag{6}$$

where, J_i represent the strength of the exchange coupling between the two-qubit, and $\hat{\sigma}_i = \{\hat{\sigma}_i^x, \hat{\sigma}_i^y, \hat{\sigma}_i^z\}, i = a, b$ are the Pauli matrices. The symmetric cross interaction Hamiltonian $\hat{\mathcal{H}}_S$ in terms of a symmetric traceless tensor Γ is defined by [13],

$$\hat{\mathcal{H}}_S = \vec{\sigma}_a.\Gamma.\vec{\sigma}_b. \tag{7}$$

The symmetric cross interaction in Eq. (7) for two-qubit system is given by,

$$\begin{aligned}\mathcal{H}_S &= \begin{pmatrix}\hat{\sigma}_a^x & \hat{\sigma}_a^y & \hat{\sigma}_a^z\end{pmatrix}\begin{pmatrix}0 & \Gamma_z & \Gamma_y\\ \Gamma_z & 0 & \Gamma_x\\ \Gamma_y & \Gamma_x & 0\end{pmatrix}\begin{pmatrix}\hat{\sigma}_b^x\\ \hat{\sigma}_b^y\\ \hat{\sigma}_b^z\end{pmatrix}\\ &= \Gamma_x\left(\hat{\sigma}_a^y\hat{\sigma}_b^z + \hat{\sigma}_a^z\hat{\sigma}_b^y\right) + \Gamma_y\left(\hat{\sigma}_a^z\hat{\sigma}_b^x + \hat{\sigma}_a^x\hat{\sigma}_b^z\right) + \Gamma_z\left(\hat{\sigma}_a^x\hat{\sigma}_b^y + \hat{\sigma}_a^y\hat{\sigma}_b^x\right).\end{aligned} \tag{8}$$

Also, $\hat{\mathcal{H}}_M$ in Hamiltonian 5 presents the magnetic field Hamiltonian model, which is defined by [8],

$$\hat{\mathcal{H}}_M = \vec{B}.(\vec{\sigma}_a + \vec{\sigma}_b), \tag{9}$$

where, $\vec{B}$ is the magnetic field vector in x, y, and z direction. Finally, the last term in the Hamiltonian 5 is the dipole–dipole interaction, which reads [5],

$$\hat{\mathcal{H}}_D = D\Big[|\vec{n}|^2\vec{\sigma}_a.\vec{\sigma}_b - 3(\vec{n}.\vec{\sigma}_a)(\vec{n}.\vec{\sigma}_b)\Big]. \tag{10}$$

where, D is the coupling of magnetic dipole–dipole interaction with $D = \frac{\mu_0\gamma^2}{16\pi|\vec{n}|^5}$ [23, 48], with μ_0 is the magnetic permeability of free space, γ is the gyro-magnetic rate, and $\vec{n}$ is the two-qubit distance vector from qubit 1 to qubit 2. In this paper, we assume the $|\vec{n}| = 1$ for different cases.

By regulating the homogeneous external magnetic field and the symmetric cross interaction in z-direction, the Hamiltonian (5) can be rewritten as,

$$\begin{aligned}\hat{H} =& J_x\hat{\sigma}_a^x\hat{\sigma}_b^x + J_y\hat{\sigma}_a^y\hat{\sigma}_b^y + J_z\hat{\sigma}_a^z\hat{\sigma}_b^z + \Gamma_z\left(\hat{\sigma}_a^x\hat{\sigma}_b^y + \hat{\sigma}_a^y\hat{\sigma}_b^x\right) + B_z(\hat{\sigma}_a^z + \hat{\sigma}_b^z) +\\ & D\Big[|\vec{n}|^2\vec{\sigma}_a.\vec{\sigma}_b - 3(\vec{n}.\vec{\sigma}_a)(\vec{n}.\vec{\sigma}_b)\Big].\end{aligned} \tag{11}$$

At thermal equilibrium, one can obtain the density operator in terms of eigensystem, where the thermal density is expressed by,

$$\rho(T) = \sum_i \lambda_i|\psi_i\rangle\langle\psi_i|, \quad \text{with the probability} \quad \lambda_i = \frac{1}{Z}e^{\frac{-E_i}{kT}}, \tag{12}$$

where, $|\psi_i\rangle$ are the eigenstates with the related eigenvalues E_i and $Z = \sum_i e^{\frac{-E_i}{kT}}$ is the partition function. The parameters T, and k are the temperature, and Boltzmann's constant, respectively. In calculations that follow we set $k = 1$.

3.1 The two dipoles are placed on the z-axis $\hat{\vec{n}} = (0, 0, 1)$

Let the dipole–dipole interaction in the z-direction, the thermal equilibrium density state (12) is calculated as,

$$\hat{\rho}_z(T) = \frac{1}{Z_1}\begin{pmatrix} A_{11} & 0 & 0 & A_{14} \\ 0 & A_{22} & A_{23} & 0 \\ 0 & A_{23} & A_{33} & 0 \\ A_{41} & 0 & 0 & A_{44} \end{pmatrix} \tag{13}$$

Where,

$$A_{11} = e^{-\frac{J_z-2D}{T}}\left(\cosh\frac{\omega_1}{T} - \frac{2B_z}{\omega_1}\sinh\frac{\omega_1}{T}\right), \quad A_{22} = e^{\frac{J_z-2D}{T}}\cosh\frac{J_x+J_y+2D}{T} = A_{33}$$

$$A_{44} = e^{-\frac{J_z-2D}{T}}\left(\cosh\frac{\omega_1}{T} + \frac{2B_z}{\omega_1}\sinh\frac{\omega_1}{T}\right), \quad A_{14} = \mu e^{-\frac{J_z-2D}{T}}\sinh\frac{\omega_1}{T} = A_{41}^*$$

$$A_{23} = -e^{\frac{J_z-2D}{T}}\sinh\frac{J_x+J_y+2D}{T}, \quad Z_1 = Tr[\hat{\rho}_z(T)]$$

$$\text{with, } \mu = \frac{J_x - J_y + 2i\Gamma_z}{\sqrt{4\Gamma_z^2 + (J_x+J_y+2D)^2}}, \text{ and, } \quad \omega_1 = \sqrt{4(\Gamma_z^2 + B_z^2) + (J_x - J_y)^2}.$$

Applying the definitions outlined in (1), 2, and 4, we aim to show a comparative investigation into the generation behaviours of entanglement, steerability, and non-locality. To achieve this, the impact of factors such as temperature, external magnetic fields, magnetic dipole, and symmetric cross interaction on the three quantum phenomena shall be analyzed and presented in Fig. 2. The two dipoles shall be applied along the z-axis for consistency. As highlighted in Fig. 2, steerability displays intermediary tendencies between non-separability and non-locality. However, both steering and non-locality violate their respective inequalities when the density state is chosen to be separable. Figure 2a–c will be utilized to showcase the three quantifiers as functions of T and D, assuming the two-qubit to be ferromagnetic materials possessing $J_x = -0.3,\ J_y = -0.7,\ J_z = -0.9$ at $\Gamma_z = 1 = B_z$. It is evident that the three quantifiers alter significantly based on temperature and the coupling of a magnetic dipole–dipole, with quantum correlations witnessing a decrease as the temperature increases. Physically, as the temperature increases, the thermal fluctuations in the environment increase. These fluctuations can cause decoherence, i.e. loss of quantum coherence in the system. Essentially, as the temperature increases, there is more noise in the system that can disrupt the delicate quantum correlations. The interaction of the magnetic dipole–dipole has a transformative effect on the material, resulting in coupling between $\hat{\sigma}_a^z\hat{\sigma}_b^z$ that is equivalent to $J_z - 2D$. Consequently, in the event that D is aligned with the negative z-axis, the material converts from a ferromagnetic substance to an anti-ferromagnetic one, and vice versa. Additionally, the upper limits of entanglement along the positive z-axis are greater than those seen for both steering and non-locality degrees, while highest quantum correlations manifest along negative D at low temperatures. This indicates that the coupling of the magnetic dipole can increase or decrease quantum correlations based on environmental and material conditions. At

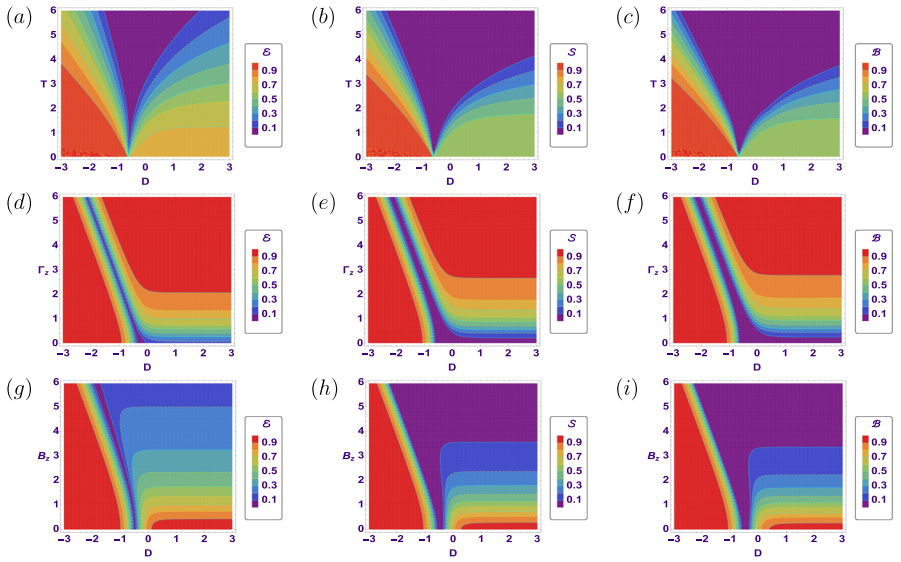

Fig. 2 The behavior of (**a**) concurrence (**b**) steering, (**c**) Bell-nonlocality, where the two dipoles are in z-direction $J_x = -0.3,\ J_y = -0.7,\ J_z = -0.9$, at $\Gamma_z = 1$, and $B_z = 1$, the functions plotted against T and D. (d,e,f) the same as (a,b,c) but the functions plotted against Γ_z and D for $T = 1$, and $B_z = 1$. (g,h,i) the same as (a,b,c) but the functions plotted against B_z and D for $T = 1$, and $\Gamma_z = 1$

higher temperatures, coupling may result in decoherence and reduce entanglement, but as the value of coupling increases, entanglement may be enhanced instead. In Fig. 2d–f, the three quantum measures are presented as functions of Γ_z and D for fixed T and B. It is noteworthy that these three quantum correlations display a symmetrical analogue in the presence of negative values of the magnetic dipole coupling. This indicates that they are unrelated to the coupling of the symmetric cross-interaction. However, in the event of positive values of the magnetic dipole–dipole coupling, the three quantum correlations heavily rely on the coupling of the symmetric cross-interaction. The phenomena in question are intensified as Γ_z increases. Generally, the symmetric cross-interaction serves to increase interaction between particles of the two-spin system. Thus, depending on the specific magnetic dipole coupling values, the impact of the symmetric cross-interaction can result in increased entanglement. The findings illustrate that the upper limits for non-separability surpass those of steering and non-locality. However, the maximum bounds for steerability exceed non-locality. The behaviour of these quantum correlations is observed to vary when plotted against the external magnetic field, as showen in Fig. 2g–i. The figs demonstrate that the strength of the external magnetic field diminishes quantumness of quantum correlations. As a result, separability increases with the increase in the external magnetic field, while steerability and non-locality diminish. Furthermore, it is observed that there are slight differences between $\mathcal{S}$ and $\mathcal{B}$, with $\mathcal{S}$ being greater than or equal to $\mathcal{B}$ in general.

3.2 The two dipoles are placed on the x-axis $\hat{\vec{n}} = (1, 0, 0)$:

Via assuming that the dipole–dipole interaction in x-direction, one can obtain the exact solution of density operator in thermal equilibrium as,

$$\hat{\rho}_x(T) = \frac{1}{Z_2}\begin{pmatrix} B_{11} & 0 & 0 & B_{14} \\ 0 & B_{22} & B_{23} & 0 \\ 0 & B_{23} & B_{33} & 0 \\ B_{41} & 0 & 0 & B_{44} \end{pmatrix} \tag{14}$$

With

$$B_{11}=e^{-\frac{J_z+D}{T}}\left(\cosh\frac{\omega_2}{T}-\frac{2B_z}{\omega_2}\sinh\frac{\omega_2}{T}\right), \quad B_{22}=e^{\frac{J_z+D}{T}}\cosh\frac{J_x+J_y-D}{T}=B_{33}$$

$$A_{44}=e^{-\frac{J_z+D}{T}}\left(\cosh\frac{\omega_2}{T}+\frac{2B_z}{\omega_1}\sinh\frac{\omega_2}{T}\right), \quad B_{14}=\xi e^{-\frac{J_z+D}{T}}\sinh\frac{\omega_2}{T}=B_{41}^{*}$$

$$B_{23}=-e^{\frac{J_z+D}{T}}\sinh\frac{J_x+J_y-D}{T}, \quad Z_2=Tr[\hat{\rho}_x(T)],$$

$$\text{with, } \xi=\frac{J_x-J_y+2i\Gamma_z}{\sqrt{4\Gamma_z^2+(J_x+J_y-D)^2}}, \text{ and, } \omega_2=\sqrt{4(\Gamma_z^2+B_z^2)+(J_x-J_y-3D)^2}.$$

Figure 3presents the behaviours of entanglement, steering, and non-locality under the influence of dipole–dipole in the x-direction, in addition to a symmetric cross interaction and an external magnetic field. Based on Fig. 3a–c, it is observed that the maximum bounds of the three phenomena at low temperatures with a magnetic dipole in the x-direction are significantly larger than those in the z-direction. However, both steering and non-locality quickly violate their inequalities as the temperature increases, particularly with positive values of the dipole coupling. This suggests that thermal fluctuations in the environment may blackuce the dipole's influence on quantum coherence. Notably, the symmetric magnetic cross interaction has a crucial contribution in enhancing non-separability, subsequently improving the steering and non-locality. This is demonstrated in Fig. 3d–f, which exhibit maximum bounds of examined quantities as the coupling of the symmetric magnetic cross interaction increases. That results suggest that the manipulation and preservation of quantum states can be facilitated with higher values of the symmetric magnetic cross interaction. In addition, the three quantifiers do not violate the hierarchy of quantum correlations. Figure 3g–i provide that it is possible to reduce the impact of a homogeneous magnetic field by increasing the coupling of the two dipoles. These findings suggest that it may be possible to neglect the aforementioned destructive effect by adjusting certain parameters of the physical system. This has important implications for the manipulation and preservation of quantum states in the presence of external magnetic fields.

Upon analyzing the results from the study illustrated in Figs. 2 and 3, it can be inferred that the quantum correlation is strongly affected with the direction of the dipole–dipole interaction. When the dipoles are oriented parallel to the symmetric cross

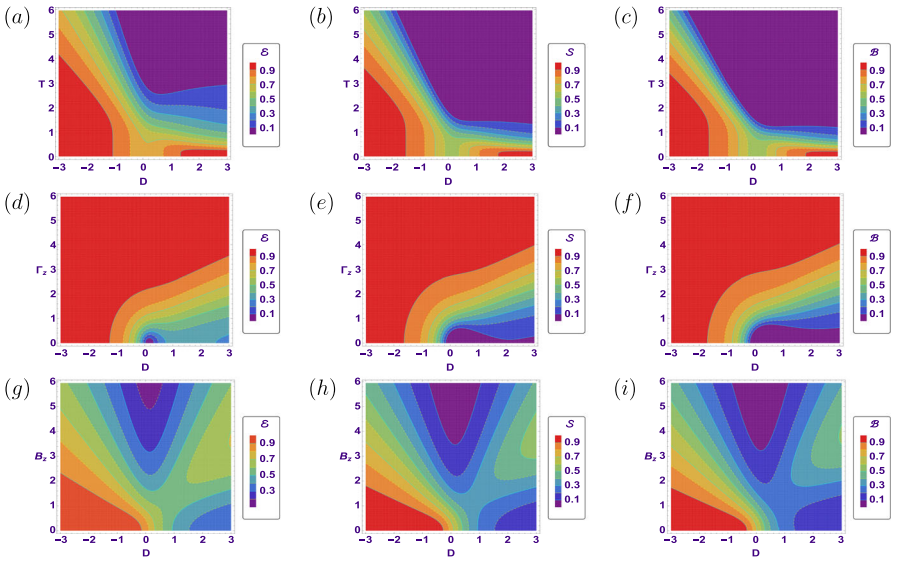

Fig. 3 The behavior of (**a**) concurrence (**b**) steering, (**c**) Bell-nonlocality, where the two dipoles are in x-direction $J_x = -0.3,\ J_y = -0.7,\ J_z = -0.9$, at $\Gamma_z = 1\ B_z = 1$, the functions plotted against T and D. (d,e,f) the same as (a,b,c) but the functions plotted against Γ_z and D for $T = 1$, $B_z = 1$. (g,h,i) the same as (a,b,c) but the functions plotted against B_z and D for $T = 1$ and $\Gamma_z = 1$

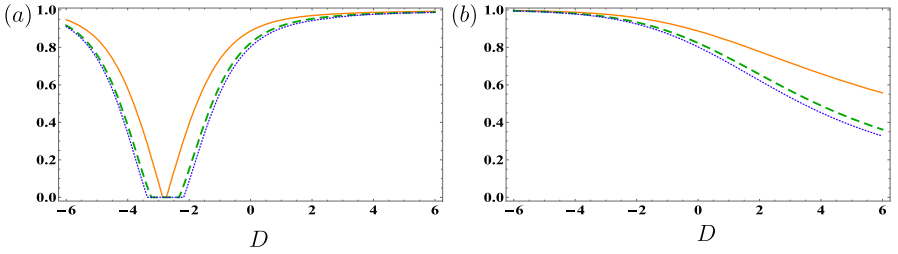

Fig. 4 The behavior of concurrence (orange-solid-curve), steering (green-dash-curve), and Bell-nonlocality (blue-dot-curve), where $J_x = -0.3,\ J_y = -0.7,\ J_z = -0.9$, at $\Gamma_z = 8$, the functions plotted against D at $B_z = 0.1$ and $T = 5$. (a) For the thermal density state (13), (b) For the thermal density state (14)

interaction field, it exhibits weaker correlation strength compared to that observed in the perpendicular direction. Furthermore, the presence of a homogeneous magnetic field reduces the strength of quantum correlation, but this effect can be mitigated by increasing the value of the dipole coupling.

To confirm the results obtained in the two previous thermal density states (13) and (14), we have plotted Fig. 4. Where we express non-separability, steering, and non-locality in two dimensions as functions of the dipole–dipole coupling. As shown, under high temperatures and negative values of the dipole coupling, the three phenomena are more pronounced there when the two dipoles are perpendicular to the other component of the system (x-direction, as depicted in Fig. 4a), as opposed to the case of the two dipoles being parallel (z-direction, as illustrated in Fig. 4b). Conversely, in cases where

the dipole coupling has positive value, findings reveal that quantum correlations attain their maximum levels when the two dipoles are parallel to the other components of the Hamiltonian. Moreover, the three forms of quantum correlation exhibit similar tendency.

3.3 The two dipoles are placed on the direction $\vec{n} = (\cos\theta, \sin\theta, 0)$

Finally, we consider the case where the external magnetic field and the symmetric cross interaction are always perpendicular to the dipole–dipole interaction. So this, we set the two dipoles in the xy-plane with the vector $\vec{n} = (\cos\theta, \sin\theta, 0)$, $\theta \in [0, 2\pi]$. Consequently, the density operator in thermal equilibrium is given by,

$$\hat{\rho}_{xy}(T) = \frac{1}{Z_3}\begin{pmatrix} \mathcal{C}_{11} & 0 & 0 & \mathcal{C}_{14} \\ 0 & \mathcal{C}_{22} & \mathcal{C}_{23} & 0 \\ 0 & \mathcal{C}_{23} & \mathcal{C}_{33} & 0 \\ \mathcal{C}_{41} & 0 & 0 & \mathcal{C}_{44} \end{pmatrix} \tag{15}$$

where,

$$\mathcal{C}_{11} = e^{-\frac{J_z+D}{T}}\left(\cosh\frac{\omega_3}{T} - \frac{2B_z}{\omega_3}\sinh\frac{\omega_3}{T}\right),$$

$$\mathcal{C}_{22} = e^{\frac{J_z+D}{T}}\cosh\frac{J_x + J_y + 2D(1-3\cos\theta)}{T} = \mathcal{C}_{33}$$

$$\mathcal{C}_{44} = e^{-\frac{J_z+D}{T}}\left(\cosh\frac{\omega_3}{T} + \frac{2B_z}{\omega_3}\sinh\frac{\omega_3}{T}\right), \quad \mathcal{C}_{14} = \eta e^{-\frac{J_z+D}{T}}\sinh\frac{\omega_3}{T} = \mathcal{C}_{41}^*$$

$$\mathcal{C}_{23} = -e^{\frac{J_z+D}{T}}\sinh\frac{J_x + J_y + 2D(1-3\cos\theta)}{T}, \quad Z_3 = Tr[\hat{\rho}_{xy}(T)],$$

$$\text{with, } \eta = \frac{-J_x + J_y + 2i(\Gamma_z - \frac{3D}{2}\sin 2\theta)}{\sqrt{4(\Gamma_z - \frac{3D}{2}\sin 2\theta)^2 + (J_x + J_y)^2}},$$

$$\text{and, } \omega_3 = \sqrt{4((\Gamma_z - \frac{3D}{2}\sin 2\theta)^2 + B_z^2) + (J_x - J_y)^2}.$$

Finally, we need to analyze the optimal position angle of a magnetic dipole with respect to the XY plane in order to determine the most significant positive impact. It is important to note that the dipole–dipole interaction always occurs perpendicular to the homogeneous magnetic field and the symmetric cross interaction, as shown in Fig. 2. In Fig. 5a–c, we assume the coupling strength of two dipoles to be positive with $D = 1$. We observe that the maximum bounds at $\theta \simeq 0,\ \pi$ in the three functions $\mathcal{E}$, $\mathcal{S}$, and $\mathcal{B}$ are greater than those shown at $\theta \simeq \pi/2,\ 3\pi/2$. These results suggest that non-separability, steerability, and non-locality are greater when the magnetic dipole is placed along the x-axis than those directed along the y-axis. It should be noted that there is a slight effect on the non-separability at $\theta \simeq \pi$ with respect to the temperature. It is observed that the non-separability, steerability, and non-locality of a dipole–dipole interaction are dependent on its orientation. Specifically, when the two dipoles are

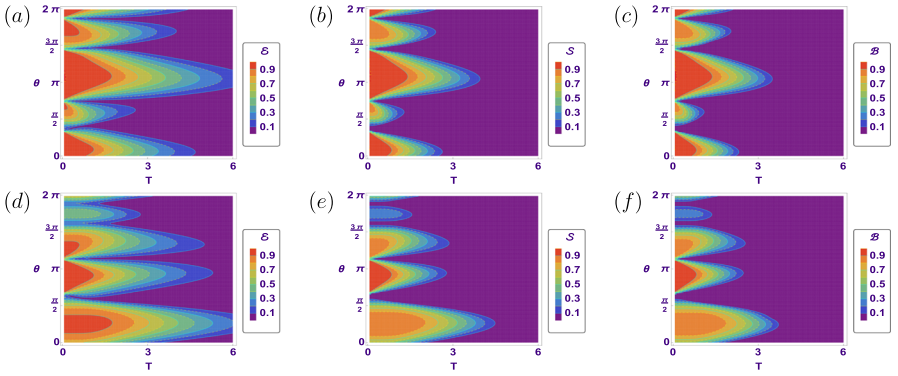

Fig. 5 The behavior of (**a**) concurrence (**b**) steering, (**c**) Bell-nonlocality, where the dipole interaction in xy-plane $J_x = -0.3,\ J_y = -0.7,\ J_z = -0.9$, at $\Gamma_z = 1\ B_z = 1\ D = 1$, the functions plotted against T and θ. (**d**–**f**) the same as (**a**–**c**) but $\Gamma_z = 1$, $B_z = 1$, and $D = -1$

aligned along the x-axis, these properties are greater than when aligned along the y-axis. Additionally, temperature has a minor impact on non-separability at an angle of approximately π. Furthermore, when the strength of the dipole–dipole interaction is negative ($D = -1$), maximum bounds of non-separability are generated at angles of approximately $\pi/4$ and π, see Fig. 5d. However, maximum bounds of steerability and non-locality are observed around an angle of π. Overall, it has been found that as the dipole angle and temperature increase, quantum correlations decrease. These findings provide valuable insights into the behaviour of our system and their quantum properties.

4 Conclusion

In this article, we presented a comprehensive comparative study that analyses the behaviour of three distinct phenomena of quantum correlations, namely non-separability, steering, and non-locality under thermal conditions. We evaluated these correlations through the implementation of a two-qubit XYZ Heisenberg chain model. We investigated the effects of symmetric cross interaction, magnetic field, and different positions of dipole–dipole interaction on each correlation. Furthermore, we analyzed the interdependence of these three phenomena of quantum correlations. Our results demonstrate that, in each case, the quantum correlation displays a similar behaviour, and there is a degree of thermal steerability existing between non-separability and non-locality. We observe that an increase in temperature and coupling of the external magnetic field leads to a reduction in the maximum bounds of the three forms of quantum correlations. Additionally, the symmetric cross interaction can improve the general behaviour of quantum correlations by minimizing unwanted effects. However, we find that the orientation of the dipole–dipole interaction plays a significant role in quantum correlation enhancement, with greater correlations being generated for the negative values of the dipole–dipole coupling compared to the positive values based

on environmental and material conditions. Our results suggest that the quantum correlations for displayed along the x-direction are superior to those displayed along the z-direction at large values of symmetric cross interaction and negative values of the coupling of the two dipoles. Therefore, regulating the magnetic dipole in a perpendicular position on the system components could enhance the quantum correlations at high temperatures and large values of symmetric cross interaction. Furthermore, the steering degree and non-locality are identical for a positive coupling of the two dipoles in the z-direction. Finally, our study substantiates a hierarchy of quantum correlations among the three types of quantum correlations for the present system.

Acknowledgements We would like to thank the referees for their important remarks which helped us to improve our results and we believe that these remarks opened some important investigates that expanded valuable improvements to the dynamics of the findings.

Author contributions The authors declare there is no conflicts of interest, financial or non-financial, for this research work presented in this manuscript.

Funding Open access funding provided by The Science, Technology & Innovation Funding Authority (STDF) in cooperation with The Egyptian Knowledge Bank (EKB).

Data availability The used code of this study is available from the corresponding author upon reasonable request.

Declarations

Conflict of interest There is no conflict of interest regarding the publication of this paper.

Ethical approval The authors declare that there is no conflict with publication ethics.

References

1. Heinrich, B., Bland, J.A.C.: Ultrathin Magnetic Structures II: Measurement Techniques and Novel Magnetic Properties, vol. 2. Springer, Cham (2006)
2. Bader, S.D.: Colloquium: opportunities in nanomagnetism. Rev. Mod. Phys. **78**, 1–15 (2006)
3. Pappas, D.P., Kämper, K.-P., Hopster, H.: Reversible transition between perpendicular and in-plane magnetization in ultrathin films. Phys. Rev. Lett. **64**, 3179–3182 (1990)
4. Ramchal, R., Schmid, A.K., Farle, M., Poppa, H.: Spiral-like continuous spin-reorientation transition of Fe/Ni bilayers on Cu(100). Phys. Rev. B **69**, 214401 (2004)
5. Rastelli, E., Regina, S., Tassi, A.: Phase transitions in a square Ising model with exchange and dipole interactions. Phys. Rev. B **73**, 144418 (2006)
6. Mól, L.A.S., Costa, B.V.: The phase transition in the anisotropic Heisenberg model with long range dipolar interactions. J. Magnet. Magn. Mater. **353**, 11–14 (2014)
7. Komatsu, H., Nonomura, Y., Nishino, M.: Temperature-field phase diagram of the two-dimensional dipolar Ising ferromagnet. Phys. Rev. E **98**, 062126 (2018)

8. Komatsu, H., Nonomura, Y., Nishino, M.: Anisotropy-temperature phase diagram for the two-dimensional dipolar Heisenberg model with and without magnetic field. Phys. Rev. B **100**, 094407 (2019)
9. Dzyaloshinsky, I.: A thermodynamic theory of "weak"ferromagnetism of antiferromagnetics. J. Phys. Chem. Solids **4**(4), 241–255 (1958)
10. Moriya, T.: Anisotropic superexchange interaction and weak ferromagnetism. Phys. Rev. **120**(1), 91 (1960)
11. Kaplan, T.A.: Single-band Hubbard model with spin-orbit coupling. Zeitschrift für Phys. B Condens. Matter. **49**(4), 313–317 (1983)
12. Shekhtman, L., Entin-Wohlman, O., Aharony, A.: Moriya's anisotropic superexchange interaction, frustration, and Dzyaloshinsky's weak ferromagnetism. Phys. Rev. Lett. **69**, 836–839 (1992)
13. Yurischev, M.A.: On the quantum correlations in two-qubit XYZ spin chains with Dzyaloshinsky-Moriya and Kaplan-Shekhtman-Entin-Wohlman-Aharony interactions. Quant. Inf. Process. **19**(9), 1–20 (2020)
14. Abd-Rabboul, M.Y., Khalil, E.M., Abdel-Khalek, S., Al-Barakaty, A., Abu-Zinadah, H.: Quantum Fisher information of a teleported state in Heisenberg XYZ chain with magnetic field and Kaplan-Shekhtman-Entin-Wohlman-Aharony interaction. IEEE Access **9**, 51325–51331 (2021)
15. Furman, G.B., Meerovich, V.M., Sokolovsky, V.L.: Entanglement of dipolar coupling spins. Quant. Inf. Process. **10**, 307–315 (2011)
16. Mahmoud Youssef Abd-Rabbou and Eied Mahmoud Khalil: Dense coding and quantum memory assisted entropic uncertainty relations in a two-qubit state influenced by dipole and symmetric cross interactions. Annalen der Physik **534**(9), 2200204 (2022)
17. Horodecki, R., Horodecki, M.: Quantum entanglement. Rev. Mod. Phys. **81**, 865 (2009)
18. Calabrese, P., Cardy, J., Tonni, E.: Entanglement negativity in quantum field theory. Phys. Rev. Lett. **109**, 130502 (2012)
19. Wootters, W.K.: Entanglement of formation and concurrence. Quant. Inf. Comput. **1**(1), 27–44 (2001)
20. Plenio, M.B.: Logarithmic negativity: a full entanglement monotone that is not convex. Phys. Rev. Lett. **95**, 090503 (2005)
21. Duarte, F. J., Taylor, T. S.: Quantum Entanglement Engineering and Applications. IOP Publishing (2021)
22. Doronin, S.I., Pyrkov, A.N., Fel'dman, É.B.: Entanglement in alternating open chains of nuclear spins s= 1/2 with the XY Hamiltonian. JETP Lett. **85**, 519–523 (2007)
23. Aldoshin, S.M., Fel'dman, E.B., Yurishchev, M.A.: Quantum entanglement and quantum discord in magnetoactive materials. Low Temp. Phys. **40**(1), 3–16 (2014)
24. Radgohar, R., Montakhab, A.: Global entanglement and quantum phase transitions in the transverse XY- Heisenberg chain. Phys. Rev. B **97**, 024434 (2018)
25. Wang, J., Landman, M., Sutter, T., Seblini, Z.: Entanglement evolution in a Heisenberg spin dimer. IEEE Trans. Magn. **55**(12), 1–3 (2019)
26. Omri, M., Abd-Rabbou, M.Y., Khalil, E.M., Abdel-Khalek, S.: Thermal information and teleportation in two-qutrit Heisenberg XX chain model. Alex. Eng. J. **61**(10), 8335–8342 (2022)
27. Abdel-Khalek, S., Khalil, E.M., Alotaibi, H., Abo-Dahab, S.M., Mahmoud, E. E., and Higazy, M: Quantum scheme of dissipative two qubits in a squeezed field: entanglement and fisher information. Alex. Eng. J., 60(3): 3411–3417 (2021)
28. Alotiabi, M. F., Khalil, E. M., and Abd-Rabbou, M. Y.: Dynamics of an atomic system associated with a cavity-optomechanical system. Res. Phys., 37: 105540 (2022)
29. Bhatt, V., Jha, P.K., Bhattacherjee, A.B., Banerjee, S.: Coherent control of quantum and entanglement dynamics via periodic modulations in optomechanical semiconductor resonator coupled to quantum-dot excitons. Quant. Inf. Process. **20**, 1–21 (2021)
30. Mohammed, N.I., Abdelsalam, H.M., Almalki, S., Abd-Rabbou, M.Y., Abdel-Khalek, S., Khalil, E.M.: Witnessing quantum correlations in two coupled quantum dots under intrinsic decoherence. Alex. Eng. J. **69**, 521–527 (2023)
31. Schrödinger, E.: Discussion of probability relations between separated systems. In: Mathematical Proceedings of the Cambridge Philosophical Society, volume 31, pp. 555–563. Cambridge University Press (1935)
32. Branciard, C., Cavalcanti, E.G., Walborn, S.P., Scarani, V., Wiseman, H.M.: One-sided device-independent quantum key distribution: security, feasibility, and the connection with steering. Phys. Rev. A **85**, 010301 (2012)

33. Saunders, D.J., Jones, S.J., Wiseman, H.M., Pryde, G.J.: Experimental EPR-steering using Bell-local states. Nat. Phys. **6**(11), 845–849 (2010)
34. Kogias, I., Lee, A.R., Ragy, S., Adesso, G.: Quantification of Gaussian quantum steering. Phys. Rev. Lett. **114**, 060403 (2015)
35. Abd-Rabbou, M.Y., Metwally, N., Ahmed, M.M.A., Obada, A.-S.F.: Decoherence and quantum steering of accelerated qubit-qutrit system. Quant. Inf. Process. **21**(10), 363 (2022)
36. Sun, W.-Y., Wang, D., Shi, J.-D., Ye, L.: Exploration quantum steering, nonlocality and entanglement of two-qubit X-state in structured reservoirs. Sci. Rep. **7**(1), 1–9 (2017)
37. Li, H.-Z., Han, R.-S., Zhang, Y.-Q., Chen, L.: Quantum steering in Heisenberg models with Dzyaloshinskii-Moriya interactions. Chin. Phys. B **27**(12), 120304 (2018)
38. Chen, L., Zhang, Y.-Q.: Quantum steering in magnetic Heisenberg models at finite temperature. EPL (Europhys. Lett.) **120**(6), 60007 (2018)
39. Abd-Rabbou, M.Y., Metwally, N., Ahmed, M.M.A., Obada, A.-S.F.: Improving the bidirectional steerability between two accelerated partners via filtering process. Modern Phys. Lett. A **37**(22), 2250143 (2022)
40. Rahman, A. U., Shamirzaie, M., and Abd-Rabbou, M. Y.: Bidirectional steering, entanglement and coherence of accelerated qubit-qutrit system with a stochastic noise. Optik, p. 170543 (2023)
41. Clauser, J.F., Horne, M.A., Shimony, A., Holt, R.A.: Proposed experiment to test local hidden variable theories. Phys. Rev. Lett. **24**, 549–549 (1970)
42. Shao-xiong, W., Zhang, J., Chang-shui, Yu., Song, H.: Uncertainty-induced quantum nonlocality. Phys. Lett. A **378**(4), 344–347 (2014)
43. Gisin, N.: Bell's inequality holds for all non-product states. Phys. Lett. A **154**(5–6), 201–202 (1991)
44. Luo, S., Shuangshuang, F.: Measurement-induced nonlocality. Phys. Rev. Lett. **106**, 120401 (2011)
45. Costa, A.C.S., Angelo, R.M.: Quantification of Einstein-Podolsky-Rosen steering for two-qubit states. Phys. Rev. A **93**, 020103 (2016)
46. Bartkiewicz, K., Horst, B., Lemr, K., Miranowicz, A.: Entanglement estimation from Bell inequality violation. Phys. Rev. A **88**, 052105 (2013)
47. Nielsen, M. A., and Chuang, I. L.: Quantum computation and quantum information (2000)
48. Kuznetsova, E.I., Yurischev, M.A.: Quantum discord in spin systems with dipole-dipole interaction. Quant. Inf. Process. **12**, 3587–3605 (2013)